Available online at www.sciencedirect.com
ScienceDirect
Journal of Photochemistry and Photobiology A: Chemistry 187 (2007) 119–126
Journal of Photochemistry and Photobiology A:Chemistry
www.elsevier.com/locate/jphotochem

Investigation of the photo-dissociation reactions for alkyl nitrite by quantum chemical molecular dynamics program "Colors-Excite"

Xiaojing Wang [a,*], Yajun Wang [b], Chen Lv [c], Momoji Kubo [c], Akira Miyamoto [c,d]

[a] *Department of Chemistry, College of Chemistry and Chemical Engineering, Inner Mongolia University, China*
[b] *College of Chemical Engineering, Inner Mongolia University of Technology, China*
[c] *Department of Applied Chemistry, Graduate School of Engineering, Tohoku University, Aoba-yama 07, Sendai 980-8579, Japan*
[d] *New Industry Creation Hatchery Center (NICHe), Tohoku University, Aoba-yama 04, Sendai 980-8579, Japan*

Received 31 March 2006; received in revised form 6 September 2006; accepted 7 October 2006
Available online 29 October 2006

Abstract

The photodissociation of alkyl nitrites series (RONO) in gaseous state were studied using density functional theory with Amsterdam Density Functional program (ADF2000) and quantum chemical molecular dynamical method by "Colors-Excite" code. The different dissociative phenomena have been explained by this investigation. Alkyl nitrites were shifted to their excited states by capturing the light energy and the bonds of O–N (RO–NO) were broken. A two-step reaction occurred for methyl nitrite (THN) to yield the diverse products, such as RO radical, NO and HNO, whereas only one-step reaction occurred for *tert*-butyl nitrite (TBN). The consistent results in theoretical calculation and experiment, including geometrical structures and excitation energies, demonstrated the good performances of "Colors-Excite".

Keywords: Photodissociation; Alkyl nitrites; Quantum chemical molecular dynamics; Density functional theory; Colors-Excite

1. Introduction

The dynamics of photo-induced reaction has been of interest to scientists working in molecular physics, spectroscopy, molecular collisions, molecular kinetics and the manufacture of new materials [1–5]. The availability of powerful lasers operating over a wide frequency range has stimulated rapid development of new experimental techniques, making it possible to analyze photodissociation processes in unprecedented detail. However, the theoretical research got far behind the experimental work. A quantitative theory of photochemical process is extremely challenging and should involve two independent ingredients: the ability to calculate molecular movement and lifetimes as well as algorithms for realistic wave-function propagation, including the transition between the ground and excited states. Thus, it is required to know the forces on atoms in the photo-excited state and the energy variation during excitation and movement. Recent advances in theory and computational methodology have made it possible to calculate the excited states and electronic absorption spectra for the system including solids, surfaces and nanostructures on the basis of the size-extensive coupled-cluster (CC) approach, the multireference configurational methods or the time-dependent Schrödinger equation [6–10]. However, because of the inherent complexity of the problems, the methods and algorithms used to compute excited states, especially the excitation dynamics, are not so efficient as the ground states, and still under development [11,12].

In the present investigation, an accelerated quantum chemical molecular dynamics code "Colors-Excite" was developed to simulate photo-induced reactions with the probe molecules of alkyl nitrites series (RONO). Alkyl nitrites have well-defined chromophore and are very light sensitive [13]. The gas-phase photodissociation of alkyl nitrites have been studied extensively for both the individual molecules and clusters [14–17]. The UV absorption spectra of the alkyl nitrites displayed two excitation bands, S_1 and S_2. It was observed that the first excitation was from the ground state into the predissociative S_1 state and S_1 band showed a vibrational progression due to the simultaneous excitation of the NO stretch mode. UV radiation dissociated alkyl nitrite into an alkoxy fragment and NO because of the

* Corresponding author. Tel.: +86 471 4344579; fax: +86 471 4992981.
E-mail address: wang_xiao_jing@hotmail.com (X. Wang).

1010-6030/$ – see front matter © 2006 Elsevier B.V. All rights reserved.
doi:10.1016/j.jphotochem.2006.10.004

weakness of ON (RO–NO) bond (∼170 kJ mol^{-1}) comparing with R–O (R–ONO) bond (∼440 kJ mol^{-1}) [18]. The processes were described with the following reaction sequence:

$$\mathrm{RONO(S_0)} + h\nu \rightarrow \ \mathrm{RONO^*(S_1)} \ \rightarrow \ \mathrm{RO(A\ or\ X)} + \mathrm{NO(X^2\Pi)} \tag{1}$$

This photodissociation had been paid close attention because alkoxy species (such as t-C_4H_9O) were important hydrocarbon intermediates in various industrial reactions [19,20]. Moreover, if alkyl nitrites on the metal surface were photo-dissociated, the alkoxy would be adsorbed on surface and NO likely desorbed due to its low binding energy [18,21,22]. It was proposed that the photodissociation of alkyl nitrite on the metal surface was likely an effective method to produce pure RO radicals. Meanwhile, it was a possible better way to study the thermochemistry of a monolayer alkoxy species without the presence of other adsorbed species. Therefore, for alkyl nitrites, the research on the process of dissociation and energy transfer caused by light energy are significant to a deeper understanding of the mechanism as well as the industrial application.

Our attention has been focused on the investigation of the reactivity and photodissociative processes for RONO in gaseous state as well as in adsorbed state by accelerated quantum chemical molecular dynamics program "Colors-Excite". As a primitive step, in this work we presented our study on the photo-induced reactions of RONO in gaseous state.

2. Computational details

The optimized structures of RONO were determined by density functional theory (DFT) employing Amsterdam Density Functional (ADF 2000 version) program package [23]. The triple-ξ Slater type orbitals (STOs) with a polarization function were applied to the valence electrons of all atoms (TZP). The Perdew and Wang's 1991 exchange and correlation function (PW91XC) was used under the generalized gradient approximation (GGA) [24]. The relativistic terms were calibrated by a combined scalar relativistic zero order regular approximation (ZORA) [25]. The excitation energies of low-lying singlet and triplet excited states were derived by the method of time-dependent density-functional theory (TDDFT) [26]. The geometries and electronic properties of excited states were further calculated using orbital occupation method by assigning the spin-α and spin-β electrons to corresponding molecular orbitals [27]. The unrestricted mode was used, which was equivalent with, in ab initio terminology, unrestricted Hartree–Fock (UHF) [28]. During the calculation of excitation energies, the van Leeuwen–Baerends (LB94) exchange and correlation potential function with the triple-zeta basis sets containing diffuse functions was used. The pictures of the optimized molecular orbitals and geometrical structures were illustrated using the molecular graphics visualization program CERIUS2 [29] and MOLEKEL4.1 [30].

An accelerated quantum chemical molecular dynamics program "Colors-Excite", which based on tight-binding approximation [31,32], was used to investigate the photodissociative reaction of alkyl nitrites. In "Colors-Excite" code, the total energy is expressed by Eq. (2):

$$E = \sum_{i=1}^{N} \frac{1}{2} m_i v_i^2 + \sum_{k=1}^{\mathrm{OCC}} \varepsilon_k + \sum_{i=1}^{N} \sum_{j>i}^{N} \frac{Z_i Z_j e^2}{R_{ij}} + \sum_{i=1}^{N} \sum_{j>i}^{N} E_{\mathrm{rep}}(R_{ij}) + E_{\mathrm{corr}} \tag{2}$$

where m_i is the atomic weight, v_i the atomic velocity, e the elementary electric charge, R_{ij} the internuclear distance, and Z_i is the atomic charge, which is evaluated by Mulliken population analysis. In Eq. (2) the first, second, third, fourth and fifth terms represent the kinetic energy of the atoms, orbital energy of the valence electrons (summation of the eigenvalues of all occupied orbitals), the Coulomb interactions between the nuclei, the short-range exchange repulsion interactions between the atoms and the energy correction relating to the excitation process, respectively. The short-range repulsion $E_{\mathrm{rep}}(R_{ij})$ and the energy correction E_{corr} is represented by Eqs. (3) and (4), respectively:

$$E_{\mathrm{rep}}(R_{ij}) = b_{ij} \ \exp\left[\frac{a_{ij} - R_{ij}}{b_{ij}}\right] \tag{3}$$

$$E_{\mathrm{corr}}(\mathrm{T}) = E_{\mathrm{corr}}(\mathrm{G}) - \{E_{\mathrm{c}}(\mathrm{G}) - E_{\mathrm{c}}(\mathrm{T})\} - \{E_{\mathrm{R}}(\mathrm{G}) - E_{\mathrm{R}}(\mathrm{T})\} - \left\{\sum \varepsilon_i(\mathrm{G}) - \sum \varepsilon_i(\mathrm{T})\right\} + \sum(\varepsilon_j - \varepsilon_i) \tag{4}$$

in which, G and T denote the ground state and triplet excited state, the parameters a and b represent the sum of the size and stiffness of atoms i and j, respectively. The first term of Eq. (3) describes the energy correction relating to the ground state. The second and third terms give the difference of the Coulomb energy and repulsion energy between ground and triplet excited state, respectively. The forth term represents the difference of the orbital energy between the corresponding ground state and triplet excited state. The last term is the energy correction produced by the excitations of the electrons from occupied orbital (i) to unoccupied orbital (j). In Eq. (4), the summations cover all the orbitals involving in the excitation. Similarly to the derivation of the Fock matrix in the unrestricted Hartree–Fock approximation, we have the following expressions for the spin-dependent Hamiltonian matrix in "Colors-Excite" code:

$$H_{\mathrm{rr}}^{\alpha} = H_{\mathrm{rr}} - \tfrac{1}{2}(P_{\mathrm{rr}}^{\alpha} - P_{\mathrm{rr}}^{\beta})(\mathrm{rr|rr}) \tag{5}$$

$$H_{\mathrm{rr}}^{\beta} = H_{\mathrm{rr}} + \tfrac{1}{2}(P_{\mathrm{rr}}^{\alpha} - P_{\mathrm{rr}}^{\beta})(\mathrm{rr|rr}) \tag{6}$$

$$H_{\mathrm{rs}}^{\alpha} = \frac{K}{2} S_{\mathrm{rs}}(H_{\mathrm{rr}} + H_{\mathrm{ss}}) - \frac{1}{2}(P_{\mathrm{rs}}^{\alpha} - P_{\mathrm{rs}}^{\beta})(\mathrm{rr|ss}) \tag{7}$$

$$H_{\mathrm{rs}}^{\beta} = \frac{K}{2} S_{\mathrm{rs}}(H_{\mathrm{rr}} + H_{\mathrm{ss}}) + \frac{1}{2}(P_{\mathrm{rs}}^{\alpha} - P_{\mathrm{rs}}^{\beta})(\mathrm{rr|ss}) \tag{8}$$

P_{ij}^{α}, P_{ij}^{β} are the full density matrix of spins α and β, respectively. H_{rr} is the diagonal term of Hamiltonian matrix, which is equal to the valence state ionization potential of each atomic orbital i ($I_i = -H_{\mathrm{rr}}$). H_{rs} is the off-Hamiltonaian and S_{rs} is the overlap matrix. We used the difference between the ionization

energy and the electron affinity energy as the one-center electron repulsion integral (rr/rr). The Nishimoto-Mataga's equation was used to calculate the two-center repulsion integral (rr/ss). In "Colors-Excite" code, the excitation is realized by transforming the electron from the occupied orbital to the corresponding empty orbital. Because Hamiltonian matrix elements are defined separately for spins α and β in Eqs. (5)–(8), the excited states of singlet and triplet multiplicity thus are calculated, respectively. The triplet state is obtained directly by assigning the same spin to two unpaired electrons. However, the mixed singlet–triplet energy is derived by assigning opposite spins to two electrons of the excited pair in our code. Therefore, Eq. (9) is used to calculate the energy of the singlet, in which E(triplet) was derived by Eqs. (10) and (11):

$$E(\text{singlet}) = 2 \times E(\text{mixed}) - E(\text{triplet}) \tag{9}$$

$$E(\text{T}) = E(\text{G}) + \Delta E \tag{10}$$

$$\begin{aligned}\Delta E = &-(\text{rrrr})_{\text{s}}\Delta n_{\alpha}(\text{s})^2 - (\text{rrrr})_{\text{p}}\Delta n_{\alpha}(\text{p})^2 - (\text{rrrr})_{\text{d}}\Delta n_{\alpha}(\text{d})^2 \\ &- (\text{rrrr})_{\text{d}}\Delta n_{\alpha}(\text{d})^2 - 2(\text{rrrr})_{\text{sp}}\Delta n_{\alpha}(\text{s})\Delta n_{\alpha}(\text{p}) \\ &-2(\text{rrrr})_{\text{sd}}\Delta n_{\alpha}(\text{s})\Delta n_{\alpha}(\text{d}) - 2(\text{rrrr})_{\text{pd}}\Delta n_{\alpha}(\text{p})\Delta n_{\alpha}(\text{d})\end{aligned} \tag{11}$$

in Eq. (11), Δn_{α}(s), Δn_{α}(p) and Δn_{α}(d) are the difference of the electron populations between ground and excited state in s, p and d orbitals, respectively. The parameters $(\text{rrrr})_i$ were fitted by reproducing the value of ΔE, which was the difference between the energies of the triplet and ground state obtained by DFT method. The optimized geometry was used to calculate the energy of the triplet state based on the consideration about the effect of the relaxed moving of the nuclei during the excitation.

In the molecular dynamical simulation by "Colors-Excite" code, the energies and the forces acting on the atoms were calculated. The atomic velocities and coordinates were updated at regular time intervals. Several properties like energy, pressure and temperature of the system can be monitored, which results in statistical averages during the simulation. The parameters, used in "Colors-Excite" code, such as the valence state ionization potential of atomic orbital i ($I_i = -H_{ii}$) and the Slater exponent of atomic orbital i, were determined precisely in the similar way with the parameterization process of our quantum chemical molecular dynamics code "Colors". The details could be referred to elsewhere [33]. The reliability of the "Colors-Excite" method has been confirmed in References [34–36]. A computer graphics code RYUGA developed in our laboratory [37] was used to visualize the three-dimensional molecular dynamical results obtained by "Colors-Excite".

3. Results and discussion

The equilibrium geometries of methyl nitrite (THN) and *tert*-butyl nitrite (TBN) were calculated using ADF2000 and "Colors-Excite" programs, respectively. For ADF2000, the optimized structure was obtained by minimizing the total energy, while for the "Colors-Excite" a dynamical simulated annealing method was used by setting up a temperature $T = 300$–1 K to get the stable equilibrium state. Fig. 1 depicted their skeleton structures. Several selected bond lengths and angles were listed in Table 1 along with the experimental values [38]. THN and TBN showed very similar structures, only the C–O bond was a little longer in TBN than in THN. The results were concordant for ADF2000 and "Colors-Excite" as well as the experimental values. The optimized structures of excited states were calculated by the same computational conditions and also listed in Table 1. The bond overlap population, which well represents the bond strength, were depicted in Fig. 2. The data of bond lengths and

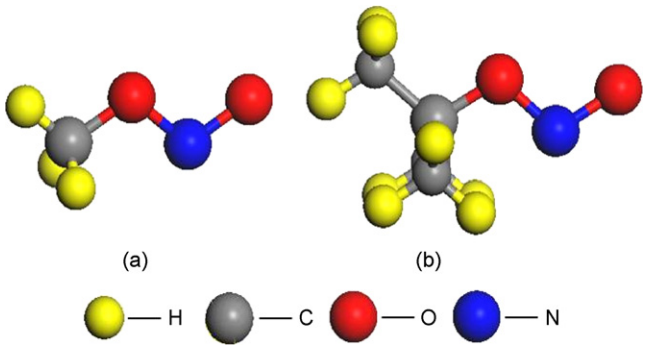

Fig. 1. Skeleton structures of (a) CH_3ONO (THN) and (b) $C(CH_3)_3ONO$ (TBN).

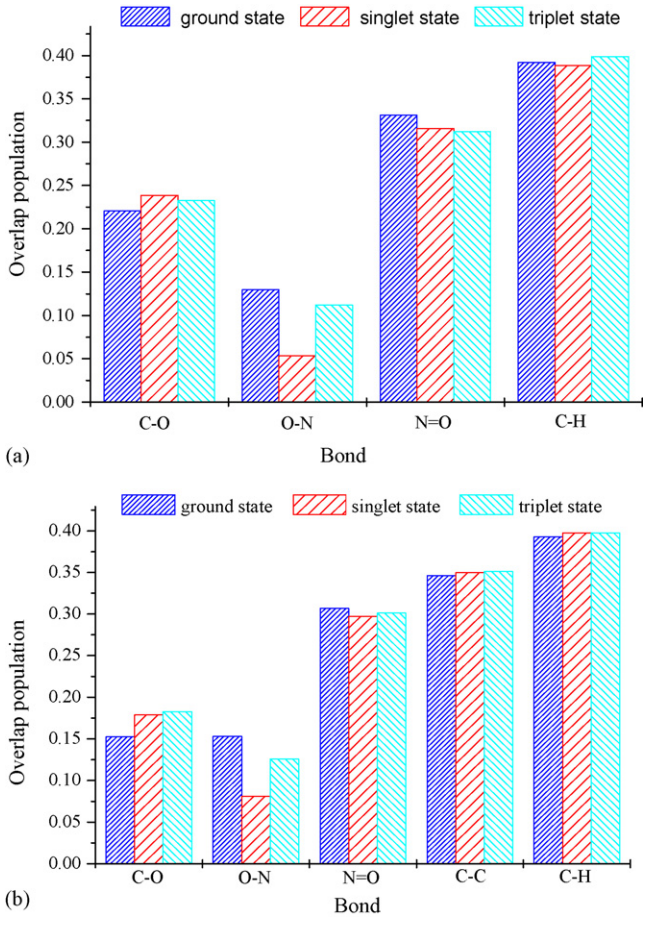

Fig. 2. Overlap populations of the ground state, singlet state and triplet state by ADF2000 program for (a) CH_3ONO (THN) and (b) $C(CH_3)_3ONO$ (TBN).

Table 1
Optimized structures of the ground state (G), singlet excited state (S) and triplet excited state (T) for CH_3ONO (THN) and $(CH_3)_3ONO$ (TBN) by ADF2000 and "Colors-Excite" methods

	ADF2000			"Colors-Excite"			Expt[38]
	G	S	T	G	S	T	G
CH_3ONO							
C–O	1.45	1.34	1.44	1.46	1.40	1.42	1.44
O–N	1.46	3.26	1.45	1.48	2.85	1.53	1.40
N–O	1.18	1.17	1.23	1.22	1.23	1.25	1.18
C–H	1.09	1.09	1.12	1.09	1.09	1.09	
C–H	1.09	1.09	1.12	1.09	1.09	1.09	
C–H	1.09	1.09	1.11	1.09	1.10	1.10	
C–O–N	109.0	108.6	78.69	122.0	158.2	163.1	114.7
O–N–O	110.7	119.4	176.8	114.0	154.7	169.0	114.8

	ADF2000			"Colors-Excite"		
	G	S	T	G	S	T
$(CH_3)_3ONO$						
C–O	1.48	1.46	1.47	1.52	1.48	1.50
O–N	1.44	1.69	1.44	1.46	1.79	1.47
N–O	1.19	1.23	1.24	1.24	1.41	1.38
C–C	1.53	1.53	1.53	1.56	1.57	1.56
C–C	1.53	1.53	1.53	1.55	1.55	1.55
C–C	1.53	1.53	1.53	1.56	1.56	1.56
C–H	1.10	1.10	1.10	1.01	1.02	1.03
C–H	1.10	1.10	1.10	1.03	1.03	1.02
C–H	1.10	1.10	1.10	1.07	1.09	1.10
C–O–N	111.6	110.4	109.6	99.9	107.0	110.8
O–N–O	110.0	117.1	119.1	92.5	96.6	98.5

overlap populations confirmed consistently that the strength of bond C–O was slightly increased from ground state to excited state, while the bond strength of N–O (RON–O) was decreased a little. The strengths of C–C and C–H bonds were nearly the same during the transition. However, the bond strength of O–N (RO–NO) in singlet state decreased largely. Therefore, it was clear that these two molecules shifted to their singlet excited state with a largely weakening of the O–N bonds after they captured the light energy.

The calculation of the vertical excitation energies and oscillator strengths were performed by the method of time-dependent density functional theory (TDDFT) (Table 2). The first vertical singlet excitation energy was 3.03 eV for THN and the maximum value was at 4.43 eV, fitting well with the experimental results of 3.10 eV and 4.13 eV, respectively [39]. For *t*-Butyl nitrite (TBN), all the excitation energies shifted to lower energies compared to methyl nitrite (THN), in which the first vertical singlet excitation energy was 1.93 eV. By analyzing the origins of the corresponding excitations in Table 2, it was found that the first excitation was from the HOMO (the highest occupied orbital) to LUMO (the lowest unoccupied orbital) for both THN and TBN, while the first strong excitation was from the HOMO − 1 (the occupied orbital next to the HOMO) to LUMO for THN and HOMO − 2 (the occupied orbital next to HOMO − 1) to LUMO for TBN. The profiles of the electron distribution in the corresponding orbitals were showed in Fig. 3, which clearly indicated that the first transition was from σ(O–N) to the first π^* antibonding orbital (primarily RO–NO), and the first strong excitation corresponded to the excitation from the lone pair of oxygen to the π^* orbital. These results confirmed that the internal coordinate subject to a significant change after the electron excitation was the O–N bond.

Based on the discussion above, a conclusion were derived that the transformation from ground state to excited state resulted in a larger change of the O–N bond in alkyl nitrites, while not much variations occurred for the other bonds. Hence, in order to understand the paths of the dissociation and to confirm the reliability of "Colors-Excite" code, we drew the potential energy surfaces of the ground state as well as the singlet and triplet excited states for THN as a function of one variable only, namely the length of the N–O bond. The result was illustrated in Fig. 4. Obviously the lowest lying singlet excited state was dissociative. That is, the molecule was changed to its singlet excited state and dissociated upon the irradiation of light energy. The onset energy of this singlet excitation were derived using the equation $E(\text{singlet}) = 2E(\text{mixed}) - E(\text{triplet})$, by calculating the triplet state and the mixed singlet–triplet, respectively. A value of 3.08 eV was obtained by "Colors-Excite", consistently with the results of TDDFT and experiment.

The complete dynamical simulations were carried out with a time step of 0.2 fs for a total time of 2000 fs. The temperature and pressure are fixed at the values of 1 01 325 Pa and 273.15 K, respectively, in the initial input data. The Verlet algorithm was used in the calculation of atomic motions. The initial model was a singlet state of RONO in which the electron was shifted to the corresponding empty orbital from an occupied orbital under the

Table 2
Vertical excitation energies (VEE, eV) and oscillator strengths (OS) for CH_3ONO (THN) and $C(CH_3)_3ONO$ (TBN) of the singlet–singlet excitations by TDDFT method

	$C(CH_3)_3ONO$ (TBN)			CH_3ONO (THN)		
	Excitation (no. of initial orbital–the no. of final orbital)	VEE	OS	Excitation (no. of initial orbital–the no. of final orbital)	VEE	OS
1	21 (HOMO)–22 (LUMO)	1.93	0.001	12 (HOMO)–13 (LUMO)	3.03	0.001
2	20 (HOMO − 1)–22 (LUMO)	2.93	0	11 (HOMO − 1)–13 (LUMO)	4.44	0.044
3	19 (HOMO − 2)–22 (LUMO)	3.98	0.029	10 (HOMO − 2)–13 (LUMO)	5.40	0
4	18 (HOMO − 3)–22 (LUMO)	4.20	0.003	9 (HOMO − 3)–13 (LUMO)	6.15	0
5	17 (HOMO − 4)–22 (LUMO), 16 (HOMO − 5)–22 (LUMO)	4.76	0.003	8 (HOMO − 4)–13 (LUMO), 12 (HOMO − 1)–14 (LUMO + 1)	7.07	0.001
6	15 (HOMO − 6)–22 (LUMO)	5.14	0	12 (HOMO − 1)–15 (LUMO + 2)	7.83	0.006
7	16 (HOMO − 5)–22 (LUMO), 17 (HOMO − 4)–22 (LUMO), 19 (HOMO − 2)–22 (LUMO)	5.26	0.072	12 (HOMO − 1)–16 (LUMO + 3), 12 (HOMO − 1)–14 (LUMO + 1)	8.12	0.043
8	14 (HOMO − 7)–22 (LUMO)	5.76	0	11 (HOMO − 1)–14 (LUMO + 1)	8.25	0.002
9	13 (HOMO − 8)–22 (LUMO)	6.18	0.010	7 (HOMO − 1)–13 (LUMO)	8.53	0.000
10	21 (HOMO)–23 (LUMO + 1)	6.53	0.008	12 (HOMO − 1)–17 (LUMO + 4), 12 (HOMO − 1)–14 (LUMO + 1)	8.82	0.214

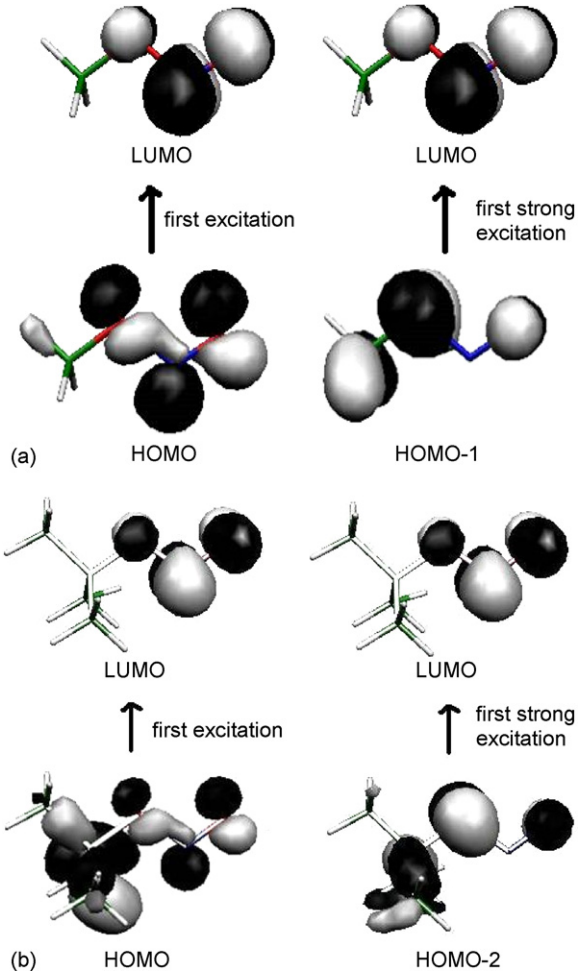

Fig. 3. Profile of the orbitals relating to the first singlet excitation and first strong singlet excitation for (a) CH_3ONO (THN) and (b) $C(CH_3)_3ONO$ (TBN).

irradiation of a 3.08 eV power. The details of photodissociation for THN and TBN were illustrated in Figs. 5 and 6 by showing snapshots of one trajectory, respectively. Fig. 5 revealed that for THN at about 800 fs, the O–N bond and then one of C–H bonds, is broken. The N–H bond was formed at about 1400 fs. Obviously, a two-step reaction occurred. The final products included NO, HNO, CH_3O and CH_2O. The routes of dissociation were showed as follows

$$CH_3ONO \xrightarrow{h\nu} CH_3O + NO \rightarrow CH_2O + HNO \quad (12)$$

However for TBN, there is no hydrogen atom in its β-site. Fig. 6 illustrated its photodissociation, in which the bond of O–N was broken at about 900 fs. Then no obvious variation was observed. Thus, only a one-step reaction occurred to yield the products of $C(CH_3)_3$ radical and NO. The process was described by Eq. (13):

$$C(CH_3)_3ONO \xrightarrow{h\nu} C(CH_3)_3O + NO \quad (13)$$

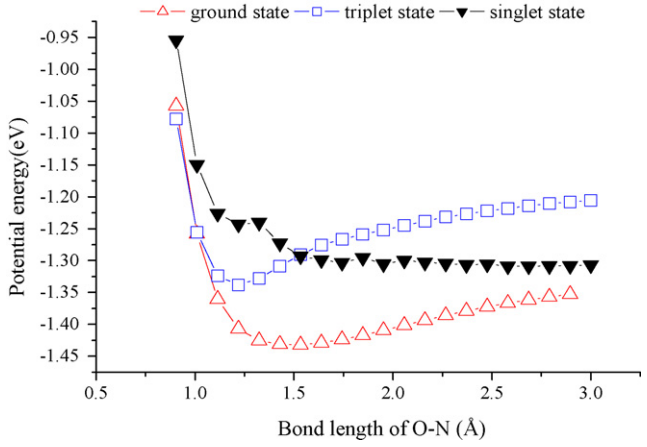

Fig. 4. Potential energy curves of the singlet and triplet state for CH_3ONO (THN) by "Colors-Excite" program.

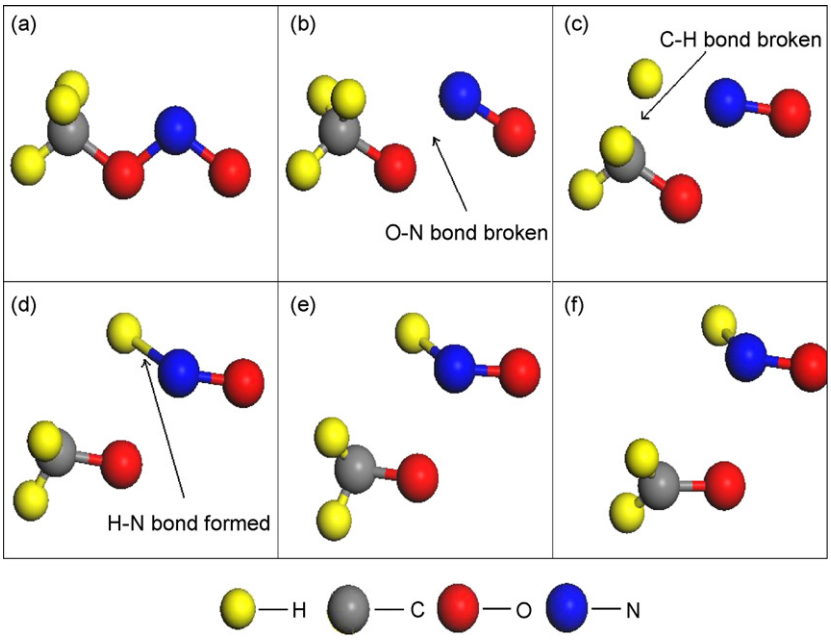

Fig. 5. Snapshots of the molecular dissociative trajectory for CH_3ONO (THN) by "Colors-Excite": (a) 0 fs, (b) 800 fs, (c) 1300 fs, (d) 1400 fs, (e) 1500 fs, and (f) 2000 fs.

The variation of bond overlap population versus reactive time during the photodissociation for THN and TBN were investigation by "Colors-Excite" program and the results were displayed in Fig. 7. The obvious variations of C–O, O–N and N–O from 600 fs to 1500 fs for THN reveal the processes of the breaking of O–N and the formation of N–H (Fig. 7a). However, the strength of the C–O bond increases, O–N and N–O bonds decrease monotonously for TBN (Fig. 7b). These results confirmed that the reactive routes were a little different for THN and TBN. The variations of the total energy versus reactive time were depicted in Fig. 8. It is clear that in the ground state of two molecules, the total energy was not varied so much with the reactive time. However, in the photodissociative state of THN (Fig. 8a), with the proceeding of the time from 500 fs to 1400 fs, the fast transformation of the energy revealed the two-step reaction occurring. A breaking of O–N bond caused the energy increasing and the forming of HNO made the system go relatively stable. As for TBN, during dissociation the energy was shifted to higher values until about 900 fs. After that time the energy decreased slowly, implying no other reactive process (Fig. 8b). In fact, the species of t-C_4H_9O has the same (C_{3V}) symmetry as CH_3O, while every β-H is replaced by CH_3. The γ-C–H bonds in t-C_4H_9O are stronger by 17 kJ mol^{-1} than the β-C–H bonds in CH_3O, which may be the possible reason that the second step of the reaction did not occur for TBN.

Table 3
Bond lengths of the final products after the photodissociation by "Colors-Excite" and the optimized structures of $C(CH_3)_3O$ and NO by ADF2000 program

"Colors-Excite" (final species of the photodissociation)				ADF2000	
				$C(CH_3)_3O$	NO
C–O	1.49	O–N	2.02	1.38 (C–O)	1.166 (ground state)
C–C	1.60	N–O	1.52	1.55 (C–C)	1.452 (excited state)
C–H	0.98			1.10 (C–H)	

The geometrical structure of the final products during the photodissociation for TBN was listed in Table 3. As a comparison, the optimized structural parameters for the species $C(CH_3)_3O$ and NO obtained by ADF2000 program were also given in

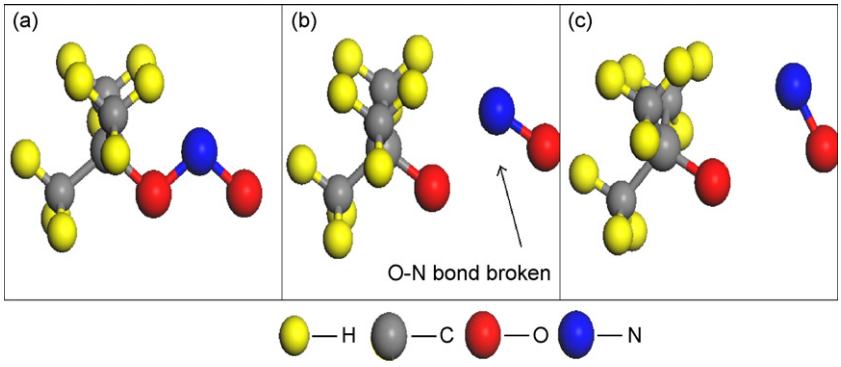

Fig. 6. Snapshots of the molecular dissociative trajectory for $C(CH_3)_3ONO$ (TBN) by "Colors-Excite": (a) 0 fs, (b) 900 fs, and (c) 2000 fs.

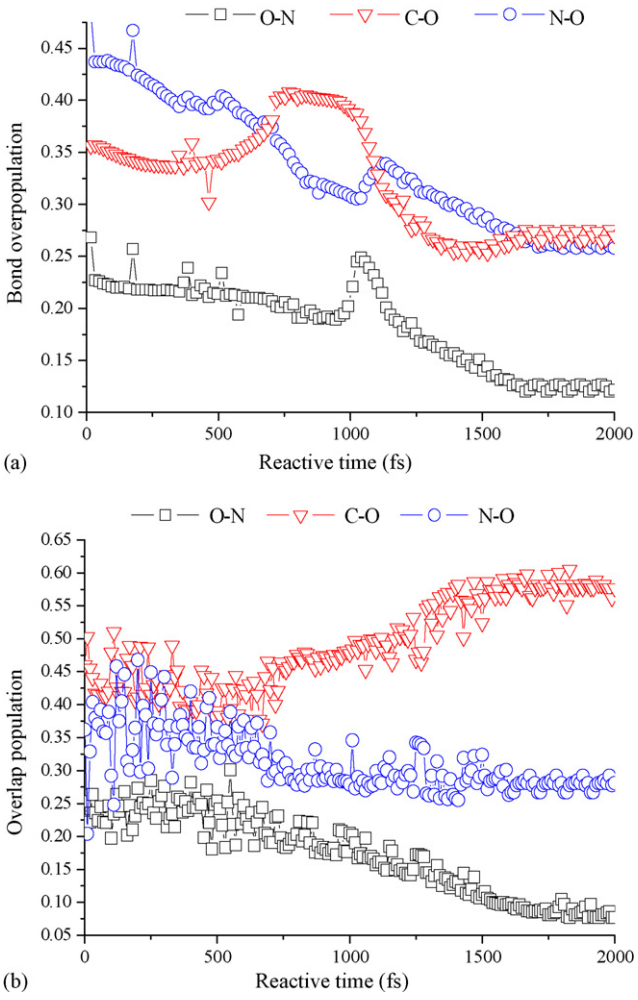

Fig. 7. Evolution of overlap populations of the bonds C–O, O–N and N–O vs. the reactive time by "Colors-Excite" for (a) CH_3ONO (THN) and (b) $C(CH_3)_3ONO$ (TBN).

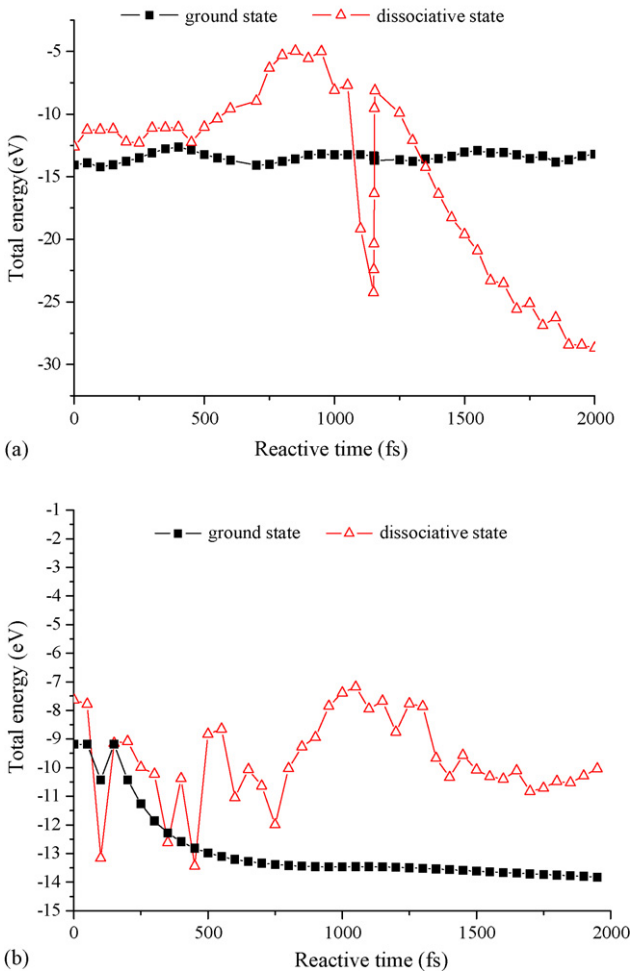

Fig. 8. Evolution of energy variation vs. the reactive time by "Colors-Excite" for (a) CH_3ONO (THN) and (b) $C(CH_3)_3ONO$ (TBN).

Table 3. The longer distance of the O–N in $C(CH_3)_3O$–NO, 2.02 Å, indicted there was no effective bonding action between $C(CH_3)_3O$ and NO species after the photodissociation. The similarity between the structure of $C(CH_3)_3O$ species formed after the dissociation by our "Colors-Excite" and the optimized structure of $C(CH_3)_3O$ by ADF2000 program demonstrated that the independent species $C(CH_3)_3O$ had been produced by the photodissociative reaction. For the NO species, it was 1.52 Å in the final products by dynamical simulation of "Colors-Excite", but the bond length in the ground state with an electronic configuration of $1\sigma^2 2\sigma^2 1\pi^4 3\sigma^2 2\pi^1$ obtained by ADF2000 was 1.12 Å. Therefore, the too longer bond length reminded us of the product NO staying at its excited state. In order to confirm it, the excited state of the NO molecule was optimized by ADF2000 and a value of bond length, 1.45 Å, was obtained for the configuration of $1\sigma^2 2\sigma^2 1\pi^4 3\sigma^1 2\pi^2$. This value was much closer to the NO species produced by the photodissociaton. It is the evidence to support the suggestion that the final NO species of photodissociative reaction staying at its higher energy state.

4. Conclusions

In this work, the photodissociative reactions of RONO in gaseous state have been investigated. The basic electronic properties were derived by the method of density functional theory. As well, the photodissociation process was simulated by a quantum chemical molecular dynamics program "Colors-Excite". The bond of O–N (RO–NO) was weakened after the excitation and the photodissociation was through the singlet state for the series of RONO. A two-step reaction occurred for CH_3ONO (THN) with a breaking of N–O bond and the formation of HNO species companying by the complex intermediate products. However, only one-step reaction existed since there are no β-C–H bonds in $C(CH_3)_3ONO$ (TBN). This investigation indicated that the alkyl nitrites (RONO) with the different alkyl group took the different photodissociative routes. The consistent results in theoretical calculation and experiment, including geometrical structures and excitation energies, demonstrated good performances of "Colors-Excite". Furthermore, the present work pointed out, by combining the density functional theory and the "Colors-Excite" code, the electronic properties and photodissociative process can be

derived accurately even for the reaction relating to the electron excitation.

References

[1] R. Schinke, Photodissociation Dynamics, Cambridge University Press, Cambridge, 1993.
[2] D. Azinovi, D. Bravo-Zhivotovskii, M. Bendikov, Y. Apeloig, B. Tumanskii, S. Vepek, Chem. Phys. Lett. 374 (2003) 257.
[3] E. Kades, M. Rosslein, J.R. Huber, J. Phys. Chem. A 101 (1997) 259.
[4] S.A. Rcid, J.T. Brandon, H. Reisler, Chem. Phys. Lett. 209 (1993) 22.
[5] H. Reisler, M. Noble, C. Witting, in: M. Ashfold, J. Baggott (Eds.), Molecular Photodissociation Dynamics, The Royal Society of Chemistry, London, 1987.
[6] T.J. Lee, G.E. Scuseria, S.R. Langhoff, Quantum Mechanical Electronic Structure Calculations with Chemical Accuracy, Kluwer, Dordrecht, 1995.
[7] O. Christiansen, H. Koch, P. Jørgensen, Chem. Phys. Lett. 243 (1995) 409.
[8] M. Wanko, M. Garavelli, F. Bernardi, T.A. Niehaus, T. Frauenheim, M. Elstner, J. Chem. Phys. 120 (2004) 1674.
[9] S. Grimme, M. Parac, Chem. Phys. Chem. 4 (2003) 292.
[10] J. Catalaĭn, J.L.G. de Paz, J. Chem. Phys. 120 (2004) 1870.
[11] M. Merchaĭn, L. Serrano-Andreĭs, Ab initio methods for excited states, in: M. Olivucci (Ed.), Computational Photochemistry, Elsevier, Amsterdam, 2005.
[12] L. Serrano-Andreĭs, M. Merchaĭn, J. Mol. Struct. Theochem. 729 (2005) 99.
[13] H. Finke, H. Spiecker, P. Andresen, J. Chem. Phys. 110 (1999) 4777.
[14] D. Schwartz-Lavi, I. Bar, S. Rosenwaks, Surf. Sci. 76 (1978) 531.
[15] E. Kades, M. Rosslein, J.R. Huber, Chem. Phys. Lett. 209 (1993) 275.
[16] K. Bergmann, J.R. Huber, J. Phys. Chem. A 101 (1997) 259.
[17] E. Kades, M. R6sslein, J.R. Huber, J. Phys. Chem. 98 (1994) 13556.
[18] H. Ihm, K. Scheer, H. Celio, J.M. White, Langmuir 17 (2001) 786.
[19] R. Schinke, S. Hennig, A. Untch, M. Nonella, J.R. Huber, J. Chem. Phys. 91 (1989) 2016.
[20] W.S. Sim, P. Gardner, D.A. King, J. Phys. Chem. 99 (1995) 16002.
[21] C.J.S.M. Simpson, P.T. Griffiths, M. Towrie, Chem. Phys. Lett. 234 (1995) 203.
[22] X.M. Yan, C. Kim, J.M. White, J. Phys. Chem. B 105 (2001) 3587.
[23] F.C. Guerra, J.G. Snijders, B. Velde, E.J. Baerends, Theor. Chem. Acc. 99 (1998) 391.
[24] J.P. Perdew, J.A. Chevary, S.H. Vosko, K.A. Jackson, M.R. Pederson, D.J. Singh, Phys. Rev. A 46 (1992) 6671.
[25] E.V. Lenthe, A.E. Ehlers, E.J. Baerends, J. Chem. Phys. 110 (1999) 8943.
[26] E.K.U. Gross, J.F. Dobson, M. Petersilka, Density Functional Theory of Time-dependent Phenomena, Springer, New York, 1996.
[27] T. Ziegler, A. Rauk, E.J. Baerends, Theor. Chim. Acta 43 (1977) 261.
[28] S.P. Karna, J. Chem. Phys. 104 (1996) 6590.
[29] Cerius2 Tutorials—Materials Science, Molecular Simulations Inc., San Diego, 1997.
[30] S. Portmann, H.P. Luthi, Chimica 54 (2000) 766.
[31] M. Elanany, P. Selvam, T. Yokosuka, S. Takami, M. Kubo, A. Imamura, A. Miyamoto, J. Phys. Chem. B 107 (2003) 1518.
[32] C. Lv, X. Wang, G. Agalya, M. Kubo, A. Miyamoto, Appl. Surf. Sci. 244 (1–4) (2005) 541.
[33] Y. Luo, P. Selvam, Y. Ito, S. Takami, M. Kubo, A. Imamura, A. Miyamoto, Organometallics 22 (2003) 2184.
[34] C. Lv, X. Wang, A. Govindasamy, M. Kubo, A. Miyamoto, Jpn. J. Appl. Phys. 44 (4B) (2005) 2806.
[35] X. Wang, C. Lv, S. Koyama, M. Kubo, A. Miyamoto, Catal. Catal. 46 (2004) 161.
[36] G. Agalya, C. Lv, X. Wang, M. Kubo, A. Miyamoto, Appl. Surf. Sci. 244 (1–4) (2005) 195.
[37] R. Miura, H. Yamano, R. Yamauchi, M. Katagiri, M. Kubo, R. Vetrivel, A. Miyamoto, Catal. Today 23 (1995) 409.
[38] P.H. Turner, M.J. Coekill, A.P. Cox, J. Phys. Chem. 83 (1979) 1473.
[39] D. Schwartz-Lavi, I. Bar, S. Rosenwaks, Chem. Phys. Lett. 128 (1986) 123.